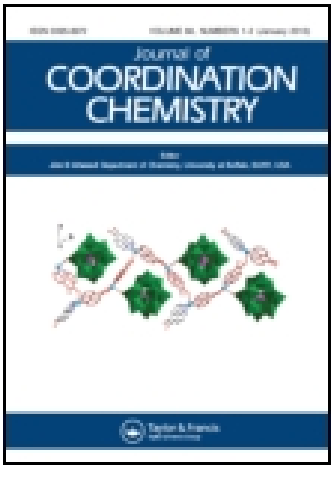

Journal of Coordination Chemistry
Publication details, including instructions for authors and subscription information:
http://www.tandfonline.com/loi/gcoo20

Synthesis, structure, and DNA-binding properties of manganese(II) and nickel(II) complexes with tris(N-ethylbenzimidazol-2-ylmethyl)amine ligand

Huilu Wu[a], Xiaoli Wang[a], Yanhui Zhang[a], Furong Shi[a], Yuchen Bai[a], Hua Wang[a] & Guolong Pan[a]

[a] School of Chemical and Biological Engineering, Lanzhou Jiaotong University, Lanzhou, PR China

Accepted author version posted online: 19 Feb 2014.Published online: 19 Mar 2014.

To cite this article: Huilu Wu, Xiaoli Wang, Yanhui Zhang, Furong Shi, Yuchen Bai, Hua Wang & Guolong Pan (2014) Synthesis, structure, and DNA-binding properties of manganese(II) and nickel(II) complexes with tris(N-ethylbenzimidazol-2-ylmethyl)amine ligand, Journal of Coordination Chemistry, 67:4, 660-669, DOI: 10.1080/00958972.2014.895823

To link to this article: http://dx.doi.org/10.1080/00958972.2014.895823

Journal of Coordination Chemistry, 2014
Vol. 67, No. 4, 660–669, http://dx.doi.org/10.1080/00958972.2014.895823

Synthesis, structure, and DNA-binding properties of manganese(II) and nickel(II) complexes with tris (N-ethylbenzimidazol-2-ylmethyl)amine ligand

HUILU WU*, XIAOLI WANG, YANHUI ZHANG, FURONG SHI, YUCHEN BAI, HUA WANG and GUOLONG PAN

School of Chemical and Biological Engineering, Lanzhou Jiaotong University, Lanzhou, PR China

(*Received 23 July 2013; accepted 16 December 2013*)

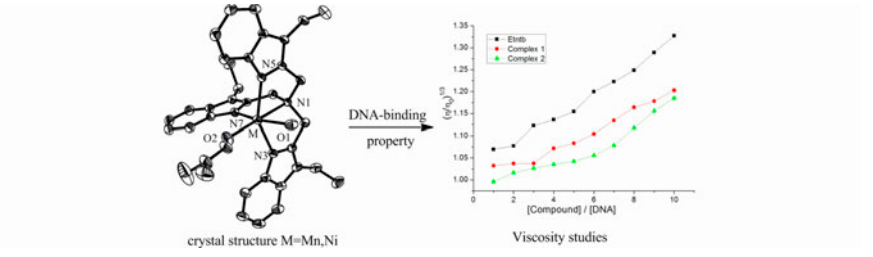

Tris(N-ethylbenzimidazol-2-ylmethyl)amine (Etntb), [Mn(Etntb)(DMF)(H_2O)](pic)$_2$ (**1**), and [Ni(Etntb)(DMF)(H_2O)](pic)$_2$ (**2**) (pic = picrate) have been synthesized and characterized by elemental analyses, molar conductivities, UV–Visible spectra, and IR spectra. Single-crystal X-ray diffraction revealed that the complexes have the same arrangement with distorted octahedral coordination geometries. DNA-binding properties of the free ligand, **1,** and **2** have been investigated by electronic absorption, fluorescence, and viscosity measurements. The results suggest that the ligand and its complexes bind DNA via intercalation, and their binding affinity for DNA follows the order **2** > **1** > ligand.

Keywords: Tris(N-ethylbenzimidazol-2-ylmethyl)amine; Mn(II) and Ni(II) complexes; Crystal structure; DNA binding

1. Introduction

Interactions of transition metal complexes with DNA have been extensively studied as DNA structural probes and DNA-dependent electron transfer probes [1, 2]. Metal complexes are used in gene regulation, mapping of protein, and DNA interaction [3]. Many

*Corresponding author. Email: wuhl@mail.lzjtu.cn

applications of these complexes require that they bind to DNA in an intercalative mode [4]. Interaction of transition metal complexes, especially those containing planar aromatic heterocyclic ligands which can insert and stack into the base pairs of DNA duplex, has attracted considerable attention [5–8].

Bis-benzimidazoles have potent activity against a number of micro-organisms, including those that lead to AIDS-related infections [9]. These compounds bind to DNA in AT-rich sequences. Benzimidazole-derived drugs have received attention owing to the fact that benzimidazole residue is a constituent of vitamin B_{12} [10], which supports potential use as therapeutics [11, 12]. Copper complexes of benzimidazole and its derivatives are of interest since they exhibit numerous biological activities such as catalase activity [13], superoxide dismutase activity, antimicrobial activity, etc. [14, 15]. As an important transition metal element, manganese can also form complexes and some manganese complexes exhibit excellent biological activities [16]. Attention has focused on the use of benzimidazole complexes as intercalating agents of DNA [17], giving valuable information to explore potential chemotherapeutical agents.

In this context, we synthesized and characterized Etntb (scheme 1), Mn(II), and Ni(II) complexes. We describe the interaction of these complexes with DNA using electronic absorption and fluorescence spectroscopy and viscosity measurements.

2. Experimental setup

2.1. *Instrumentation*

The C, H, and N elemental analyses were determined using a Carlo Erba 1106 elemental analyzer. Electrolytic conductance measurements were made with a DDS-11A type conductivity bridge using a 10^{-3} M L^{-1} solution in DMF at room temperature. IR spectra were recorded from 4000 to 400 cm^{-1} with a Nicolet FT-VERTEX 70 spectrometer using KBr pellets. Electronic spectra were taken on a Lab-Tech UV Bluestar spectrophotometer. Fluorescence spectra were recorded on a 970-CRT spectrofluorophotometer.

2.2. *Materials and methods*

Calf thymus DNA (CT-DNA) and ethidium bromide (EB) were purchased from Sigma Aldrich Chemicals Co. (USA). All chemicals used were of analytical grade. Stock solution of ligand and complexes were dissolved in DMF at 3×10^{-3} M. All experiments involving

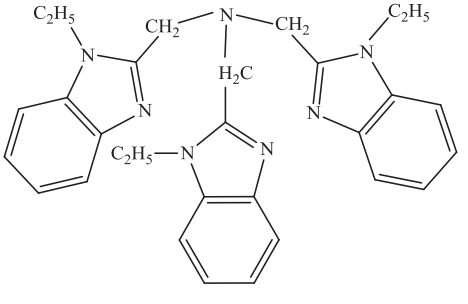

Scheme 1. Structure of Etntb.

interaction of the ligand and complexes with CT-DNA were carried out in doubly distilled water buffer containing 5 mM Tris and 50 mM NaCl and adjusted to pH 7.2 with hydrochloric acid. A solution of CT-DNA gave a ratio of UV absorbance at 260 and 280 nm of 1.8–1.9, indicating that the CT-DNA was sufficiently free of protein [18]. The CT-DNA concentration per nucleotide was determined spectrophotometrically by employing an extinction coefficient of 6600 M^{-1} cm^{-1} at 260 nm [19].

Absorption titration experiment was performed with fixed concentrations of the complexes while gradually increasing the concentration of CT-DNA. While measuring the absorption spectra, a proper amount of CT-DNA was added to both compound solution and the reference solution to eliminate the absorbance of CT-DNA itself. From the absorption titration data, the binding constant was determined using [20].

$$[\mathrm{DNA}]/(\varepsilon_a - \varepsilon_f) = [\mathrm{DNA}]/(\varepsilon_b - \varepsilon_f) + 1/K_b(\varepsilon_b - \varepsilon_f)$$

where [DNA] is the concentration of CT-DNA in base pairs, ε_a corresponds to the extinction coefficient observed (A_{obsd}/[M]), ε_f corresponds to the extinction coefficient of the free compound, ε_b is the extinction coefficient of the compound when fully bound to CT-DNA, and K_b is the intrinsic binding constant. The ratio of slope to intercept in the plot of $[\mathrm{DNA}]/(\varepsilon_a - \varepsilon_f)$ *versus* [DNA] gives K_b.

EB emits intense fluorescence in the presence of CT-DNA, due to its strong intercalation between adjacent CT-DNA base pairs. The enhanced fluorescence can be quenched by addition of a second molecule [21, 22]. The quenching extent of fluorescence of EB bound to CT-DNA is used to determine the extent of binding between the second molecule and CT-DNA. CT-DNA competitive binding with EB was carried out in the buffer by keeping [DNA]/[EB] = 1 and varying the concentrations of the compounds. The fluorescence spectra of EB were measured using excitation wavelength at 520 nm and emission range set between 550 and 750 nm. The spectra were analyzed according to the classical Stern–Volmer equation [23],

$$I_0/I = 1 + K_{sv}r$$

where I_0 and I are the fluorescence intensities at 599 nm in the absence and presence of the compounds, respectively, K_{sv} is the linear Stern–Volmer quenching constant, and r is the ratio of the total concentration of the compounds to that of CT-DNA ([compound]/[DNA]). ([CT-DNA] = 2.5×10^{-3} M L^{-1}, [EB] = 2.2×10^{-3} M L^{-1}).

Viscosity experiments were conducted on an Ubbelodhe viscometer, immersed in a thermostated water bath at 25 ± 0.1 °C. Titrations were performed for the complexes (3 mM), and each compound was introduced into CT-DNA solution (50 μM) present in the viscometer. Data were presented as $(\eta/\eta_0)^{1/3}$ *versus* the ratio of the concentration of the compound to CT-DNA, where η is the viscosity of CT-DNA in the presence of the compound and η_0 is the viscosity of CT-DNA alone. Viscosity values were calculated from the observed flow time of CT-DNA containing solution corrected from the flow time of buffer alone (t_0), $\eta = (t - t_0)/t_0$ [24].

2.3. *Preparation of the ligand Etntb*

The compound was synthesized by the literature method [25] and characterized by ^{1}H NMR spectroscopy. Yield: 5.2 g (63%). The ^{1}H NMR spectrum of Mentb was consistent with the literature [26]. ^{1}H NMR ($CDCl_3$) δ/ppm: 0.76 (t, 9H, CH_3), 3.46 (q, 6H, CH_2),

4.28 (s, 6H, *H*1), 7.22 (m, 9H, *H*3–5), 7.74 (dd, 3H, *H*2). UV–Vis (λ, nm): 287, 279. IR (selected data, KBr, cm^{-1}): $v = 1276$ (ν_{C-N}), 1509 ($\nu_{C=N}$), 1463 ($\nu_{C=N-C=C}$) stretching frequency, respectively.

2.4. *Preparation of the complexes*

2.4.1. [Mn(Etntb)(DMF)(H_2O)](pic)$_2$ (1). To a stirred solution of Etntb (0.0982 g, 0.2 mM) in hot MeOH (10 mL) was added to a solution of Mn(pic)$_2$ (0.102 g, 0.2 mM) in MeOH (5 mL). A yellow crystalline product formed rapidly. The precipitate was filtered off, washed with MeOH and absolute Et_2O, and dried in vacuo. The dried precipitate was dissolved in DMF to form a yellow solution that was allowed to have Et_2O diffused at room temperature. Yellow crystals of [Mn(Etntb)(DMF)(H_2O)](pic)$_2$ (**1**) suitable for X-ray measurement were obtained after three weeks. Calcd (%) for **1** $C_{45}H_{46}MnN_{14}O_{16}$ (MW 1093.90): C, 49.41; H, 4.24; N, 17.93. Found: C, 49.37; H, 4.21; N, 17.97. Λ_m(DMF, 297 K): 128 S cm^2 M^{-1}. UV–Vis (λ, nm): 370, 389. IR (selected data, KBr, cm^{-1}): $v = 1267$(ν_{C-N}), 1490 ($\nu_{C=N}$), 1452 ($\nu_{C=N-C=C}$).

2.4.2. [Ni(Etntb)(DMF)(H_2O)](pic)$_2$ (2). The Ni(II) complex (**2**) was prepared by the same method. Anal. (%) Calcd for **2** $C_{45}H_{46}NiN_{14}O_{16}$ (MW 1097.67): C, 49.24; H, 4.22; N, 17.87. Found: C, 49.27; H, 4.18; N, 17.93. Λ_m(DMF, 297 K): 129 S cm^2 M^{-1}. UV–Vis (λ, nm): 369, 399. IR (selected data, KBr, cm^{-1}): $v = 1263$ (ν_{C-N}), 1497 ($\nu_{C=N}$), 1453 ($\nu_{C=N-C=C}$).

Table 1. Crystallographic data and data collection parameters for **1** and **2**.

Complex	**1**	**2**
Molecular formula	$C_{45}H_{46}MnN_{14}O_{16}$	$C_{45}H_{46}N_{14}O_{16}Ni$
Molecular weight	1093.90	1097.67
Crystal system	Triclinic	Triclinic
Space group	*P-1*	*P-1*
a (Å)	12.1937(12)	12.3530(13)
b (Å)	12.9613(12)	12.7912(13)
c (Å)	16.6798(16)	16.2060(16)
α (°)	108.461 (2)	108.3970(10)
β (°)	93.355(2)	94.4910(10)
γ (°)	97.513(2)	97.8730(10)
V (Å^3)	2465.0(4)	2386.7(4)
Z	2	2
ρ_{Calcd} (mg m^{-3})	1.474	1.527
Absorption coefficient (mm^{-1})	0.354	0.495
F (0 0 0)	1134	1140
Crystal size (mm)	0.35 × 0.32 × 0.23	0.28 × 0.21 × 0.11
θ range for data collection (°)	1.75–25.00	1.68–25.00
h/k/l (max, min)	−11,14/−15,11/−19,19	−14,14/−14,15/−19,19
Reflections collected	12,706	17,220
Independent reflections	8617 [*R*(int) = 0.0229]	8331 [*R*(int) = 0.0247]
Refinement method	Full-matrix least-squares on F^2	Full-matrix least-squares on F^2
Data/restraints/parameters	8617/828/693	8331/0/705
Goodness-of-fit on F^2	1.048	1.393
Final R_1, wR_2 indices [$I > 2\sigma(I)$]	0.0504, 0.1278	0.0342, 0.0847
R_1, wR_2 indices (all data)	0.0814, 0.1392	0.0370, 0.0858
Largest differences peak and hole (eÅ^{-3})	0.633 and −0.442	0.706 and −0.426

2.5. *X-ray crystallography*

A suitable single crystal was mounted on a glass fiber and the intensity data were collected on a Bruker Smart CCD diffractometer with graphite-monochromated Mo Kα radiation (λ = 0.71073 Å) at 293 K. Data reduction and cell refinement were performed using SMART and SAINT [27]. The structure was solved by direct methods and refined by full-matrix least squares against F^2 of data using SHELXTL [28]. All hydrogens were found in difference electron maps and were subsequently refined in a riding model approximation with C–H distances ranging from 0.95 to 0.99 Å. Basic crystal data, description of the diffraction experiment, and details of the structure refinement are given in table 1.

3. Results and discussion

The two complexes are soluble in DMF and DMSO but insoluble in water and organic solvents, such as methanol, ethanol, petroleum ether, trichloromethane, etc. The elemental analyses show that the compositions are [Mn(Etntb)(DMF)(H_2O)](pic)$_2$ and [Ni(Etntb)(DMF)(H_2O)](pic)$_2$. A comparison of molar conductance values shows 1 : 2 electrolytes of the complex in DMF [29].

DMF solutions of the ligand and its complexes show, as expected, almost identical UV spectra. The UV bands of the ligand (287, 279 nm) are only marginally blue-shifted (3–5 nm) in the complexes, evidence of C=N coordination. These bands are assigned to $\pi\rightarrow\pi^*$ (imidazole) transitions. The picrate bands (observed at 370, 389 nm for **1** and 369, 399 nm for **2**) are assigned to $n\rightarrow\pi^*$ and $\pi\rightarrow\pi^*$ transitions.

IR spectra of **1** and **2** are closely related to that of free Etntb. One of the most diagnostic changes occurs at 1500 and 1270 cm^{-1}. The spectrum of ligand shows a strong band at 1463 cm^{-1} and two weak bands at 1276 and 1509 cm^{-1}. By analogy with the assigned bands of imidazole, the former can be attributed to (C=N–C=C), while the latter can be attributed to (C=N) and (C–N). The location of the three bands slightly shifted for **1** to lower frequencies [30]. The band at 1463 cm^{-1} is shifted to 1452 cm^{-1}, which can be attributed to the coordination of benzimidazole nitrogen. Similar shifts also appear in **2**, giving the same conclusion.

3.1. *X-ray structure determination of 1 and 2*

The molecular structures of **1** and **2** are shown in figure 1. Selected bond lengths and angles of **1** and **2** are listed in table 2.

As shown in figure 1, the crystal structure of the two complexes consists of discrete [M(Etntb)·DMF·H_2O]$^{2+}$ and two picrates. The metals are six-coordinate with a MN_4O_2 chromophore, and the coordination sphere around M(II) is distorted octahedral. The ligand is a tetradentate N-donor, with the remaining coordination sites on M occupied by water and DMF. In **1**, the manganese is 0.619 Å above the basal plane N3–N5–N7, but in **2**, the nickel is 0.358 Å above the basal plane N3–N5–N7. The DMF is accommodated at the open axial site without any significant change in the pseudo-octahedral geometry of the complexes (average N1–M–NA for **1** is 91.47° and **2** is 97.37°). In the dichloro complex Mn^{II}(ntb)Cl_2, a sixth ligand, the chloride, opens one site of the trigonal basal plane to form a square basal plane (NB–Mn–NB = 143.1°) [31]. When a sixth ligand is coordinated to the

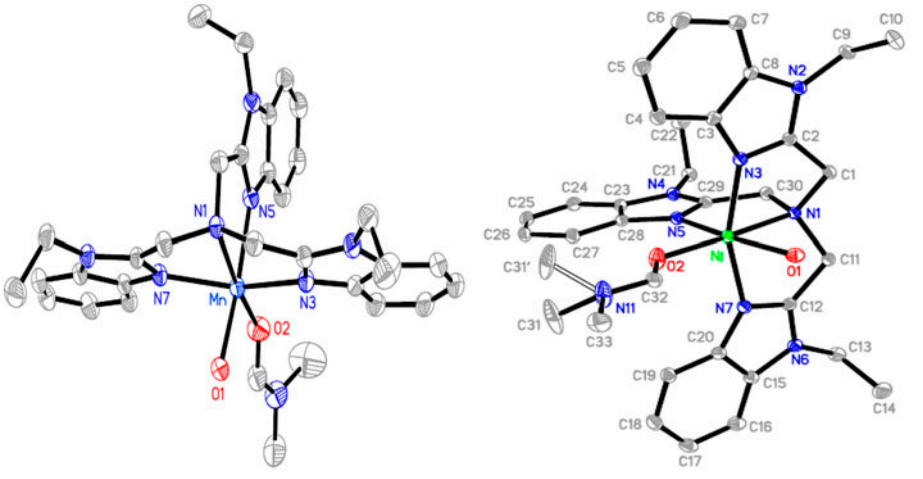

Figure 1. The molecular structures of **1** and **2** showing displacement ellipsoids at the 30% probability level. Hydrogens and anions have been omitted for clarity.

Table 2. Selected bond lengths (Å) and angles (°) of **1** and **2**.

Complexes	**1**		**2**	
Bond distances	Mn–N(1)	2.440(2)	Ni–N(1)	2.1890(16)
	Mn–N(3)	2.215(2)	Ni–N(3)	2.0641(16)
	Mn–N(5)	2.189(2)	Ni–N(5)	2.0505(16)
	Mn–N(7)	2.200(2)	Ni–N(7)	2.0738(16)
	Mn–O(1)	2.197(2)	Ni–O(1)	2.0998(15)
	Mn–O(2)	2.120(2)	NiO–(2)	2.0679(14)
Bond angles	N(1)–Mn–N(3)	74.08(8)	N(1)–Ni–N(3)	79.21(6)
	N(1)–Mn–N(5)	76.18(8)	N(1)–Ni–N(5)	82.09 (6)
	N(1)–Mn–N(7)	73.00(7)	N(1)–Ni–N(7)	80.66(6)
	N(1)–Mn–O(1)	87.75(8)	N(1)–Ni–O(1)	88.64(6)
	N(1)–Mn–O(2)	174.46(8)	N(1)–Ni–O(2)	176.16(6)
	O(1)–Mn–O(2)	96.72(9)	O(1)–Ni–O(2)	95.19(6)

metal complex of a tripodal tetradentate ligand, the geometry of the three benzimidazole nitrogens may be retained, while the complex changes its geometry from trigonal bipyramidal to partial trigonal pyramidal; alternatively, the geometry of the three benzimidazole nitrogens may change from trigonal basal to square basal to accommodate the new ligand with the complex changing its geometry from trigonal bipyramidal to octahedral.

3.2. *DNA-binding experiments*

3.2.1. Electronic absorption titration. The binding interaction of metal complexes (not only of nickel) with different ligands has been investigated [32]. Electronic absorption spectroscopy has been widely employed to determine the binding characteristics of metal complexes with DNA [33–35]. Absorption spectra of the free ligand, **1**, and **2** in the absence and presence of CT-DNA (at a constant concentration of complex) are given in figure 2. With increasing DNA concentrations, the hypochromisms are 19.6% at 276 nm for free

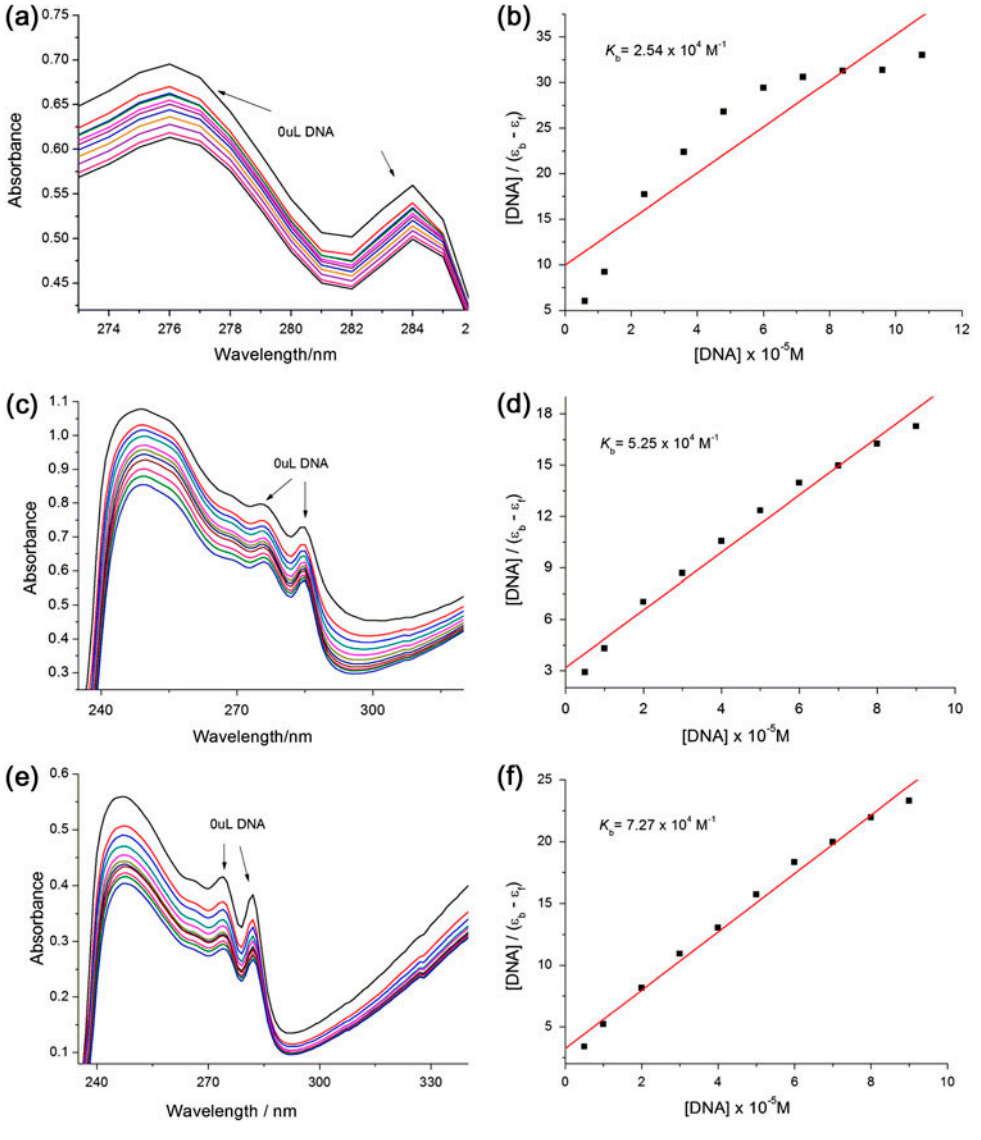

Figure 2. Electronic spectra of free Etntb (a), **1** (c) and **2** (e) in Tris–HCl buffer upon addition of CT-DNA. [Compound] = 3×10^{-5} M, [DNA] = 2.5×10^{-3} M. The arrow shows the emission intensity changes upon increasing DNA concentration. Plots of [DNA]/($\varepsilon_a - \varepsilon_f$) *vs.* [DNA] for titration of ligand (b), **1** (d), and **2** (f) with CT-DNA.

Etntb, 21.5% at 275 nm for **1**, and 30.2% at 282 nm for **2**. The λ_{max} for free Etntb increased from 276 to 277, which for **1** increased from 275 to 277 nm and that for **2** increased from 282 to 283 nm, i.e. a slight red shift of about 1–2 nm under identical experimental conditions. The hypochromism and red shift suggest that the compounds interact with CT-DNA [36]. The K_b values of free Etntb, **1** and **2** were $(2.54 \pm 0.024) \times 10^4\ M^{-1}$ ($R = 0.97$ for 7 points), $(5.25 \pm 0.048) \times 10^4\ M^{-1}$ ($R = 0.98$ for 10 points), and $(7.27 \pm 0.031) \times 10^4\ M^{-1}$

($R = 0.96$ for 10 points), respectively. Hence, the binding strength of **2** is greater than that of **1** and the free ligand.

3.2.2. Competitive binding with EB. In general, measurement of the ability of a complex to affect the EB fluorescence intensity in the EB-DNA adduct allows determination of the affinity of the complex for DNA, whatever the binding mode may be. If a complex replaces EB from DNA-bound EB, the fluorescence of the solution will be quenched due to the fact that free EB molecules are readily quenched by water [37]. For the compounds, no emission was observed either alone or in the presence of CT-DNA in the buffer. Addition of Etntb does not provoke any significant changes of intensity or position of the emission band at 599 nm of the DNA-EB system, indicating that free Etntb cannot replace EB from the DNA-EB complex. The fluorescence quenching of EB bound to CT-DNA by **1** and **2** is shown in figure 3. The quenching of EB bound to CT-DNA by both complexes is in agreement with the linear Stern–Volmer equation, which provides further evidence that the complexes bind to DNA. The K_{sv} values for **1** and **2** are $(1.69 \pm 0.07) \times 10^3\ M^{-1}$ ($R = 0.96$ for 5 points) and $(4.00 \pm 0.01) \times 10^3\ M^{-1}$ ($R = 0.95$ for 11 points), respectively. The data suggest that the interaction of **2** with CT-DNA is stronger than that of **1**, which is consistent with the above absorption spectral results. The Kq values for the Mn(II) and Ni(II) complexes are 1.69×10^{11} and $4.00 \times 10^{11}\ L\ M^{-1}\ S^{-1}$, so they are static quenching [38].

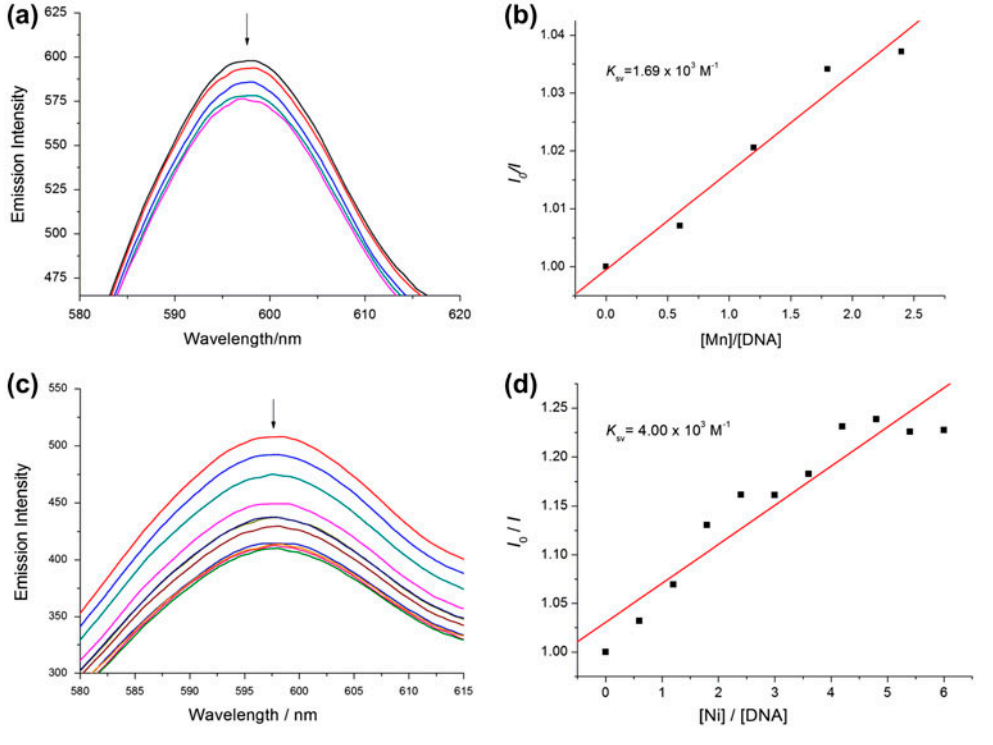

Figure 3. Emission spectra of EB bound to CT-DNA in the presence of **1** (a) and **2** (c). [Complex] = 3×10^{-3} M; $\lambda_{ex} = 520$ nm. The arrows show the intensity changes upon increasing concentrations of the complexes. Fluorescence quenching curves of EB bound to CT-DNA by **1** (b) and **2** (d). (Plots of I_0/I *vs.* [Complex].)

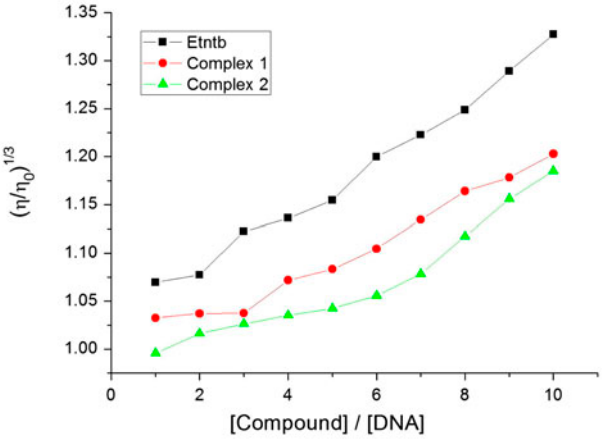

Figure 4. Effect of increasing amounts of the compounds on the relative viscosity of CT-DNA at 25.0 ± 0.1 °C.

3.2.3. Viscosity studies. Optical photophysical probes generally provide necessary but not sufficient clues to support a binding model. Measurements of DNA viscosity that are sensitive to DNA length are regarded as the least ambiguous and the most critical tests of binding in solution in the absence of crystallographic structural data [39, 40]. We have therefore carried out DNA viscosity measurements. The values of $(\eta/\eta_0)^{1/3}$ were plotted against [compound]/[DNA] (figure 4). Upon addition of **1**, **2,** and free ligand, the viscosity of rod-like CT-DNA increased significantly, which suggests that Etntb and its complexes can all bind to DNA by intercalation [41].

4. Conclusion

Mn(II) and Ni(II) complexes of Etntb have been synthesized and characterized. The DNA-binding properties of these compounds were investigated by electronic absorption, fluorescence, and viscosity measurements. The results indicate that the ligand, **1**, and **2** can bind to CT-DNA, by intercalation, and their affinity to DNA follows the order **2** > **1** > Etntb. These results should be proved useful in designing of probes of nucleic acid structures.

Supplementary material

Crystallographic data (excluding structure factors) for the structures reported in this article have been deposited with the Cambridge Crystallographic Data Center with reference numbers CCDC 825136 and 825137. Copies of the data can be obtained free of charge on application to the CCDC, 12 Union Road, Cambridge CB2 1EZ, UK. Tel. +44 01223 762 910; Fax: +44 01223 336 033; E-mail: deposit@ccdc.cam.ac.uk or http://www.ccdc.cam.ac.uk.

Funding

The present research was supported by the National Natural Science Foundation of China [grant number 21367017]; the Fundamental Research Funds for the Gansu Province Universities [grant number 212086]; National Natural Science Foundation of Gansu Province [grant number 1212RJZA037]; and “Qing Lan” Talent Engineering Funds for Lanzhou Jiaotong University.

References

[1] K.E. Erkkila, D.T. Odom, J.K. Barton. *Chem. Rev.*, **99**, 2777 (1999).
[2] C. Metcalfe, J.A. Thomas. *Chem. Soc. Rev.*, **32**, 215 (2003).
[3] B. Li, W. Liu, J. Shao, C.L. Xue, C.Z. Xie, Y. Ouyang, J.Y. Xu. *J. Coord. Chem.*, **66**, 2465 (2013).
[4] L.M. Chen, J. Liu, J.C. Chen, S. Shi, C.P. Tan, K.C. Zheng, L.N. Ji. *J. Mol. Struct.*, **881**, 156 (2008).
[5] W. Lewandowski, M. Kalinowska, H. Lewandowska. *J. Inorg. Biochem.*, **99**, 1407 (2005).
[6] R. Chen, C.S. Liu, H. Zhang, Y. Guo, X.H. Bu, M. Yang. *J. Inorg. Biochem.*, **101**, 412 (2007).
[7] E.R. Jamieson, S.J. Lippard. *Chem. Rev.*, **99**, 2467 (1999).
[8] W.K. Pogozelski, T.D. Tullius. *Chem. Rev.*, **98**, 1089 (1998).
[9] C.A. Bell, C.C. Dykstra, N.A. Naiman, M. Cory, T.A. Fairley, R.R. Tidwell. *Antimicrob. Agents Chemother.*, **37**, 2668 (1993).
[10] D.J. Skalitzky, J.T. Marakovits, K.A. Maegley, A. Ekker, X.-H. Yu, Z. Hostomsky, S.E. Webber, B.W. Eastman, R. Almassy, J. Li, N.J. Curtin, D.R. Newell, A.H. Calvert, R.J. Griffin, B.T. Golding. *J. Med. Chem.*, **46**, 210 (2003).
[11] J.P. Lalezari, J.A. Aberg, L.H. Wang, M.B. Wire, R. Miner, W. Snowden, C.L. Talarico, S. Shaw, M.A. Jacobson, W.L. Drew. *Antimicrob. Agents Chemother.*, **46**, 2969 (2002).
[12] N.H. Hauel, H. Nar, H. Priepke, U. Ries, J.-M. Stassen, W. Wienen. *J. Med. Chem.*, **45**, 1757 (2002).
[13] M. Devereux, D.O. Shea, A. Kellett, M. McCann, M. Walsh, D. Egan, C. Deegan, K. Kędziora, G. Rosair, H. Müller-Bunz. *J. Inorg. Biochem.*, **101**, 881 (2007).
[14] M. Devereux, D. O'Shea, M. O'Connor, H. Grehan, G. Connor, M. McCann, G. Rosair, F. Lyng, A. Kellett, M. Walsh, D. Egan, B. Thati. *Polyhedron*, **26**, 4073 (2007).
[15] F. Arjmand, B. Mohani, S. Ahmad. *Eur. J. Med. Chem.*, **40**, 1103 (2005).
[16] E.J. Gao, Y. Zhang, L. Lin, R.S. Wang, L. Dai, Q. Liang, M.C. Zhu, M.L. Wang, L. Liu, W.X. He, Y.J. Zhang. *J. Coord. Chem.*, **64**, 3992 (2011).
[17] C.Y. Zhou, J. Zhao, Y.B. Wu, C.X. Yin, Y. Pin. *J. Inorg. Biochem.*, **101**, 10 (2007).
[18] S. Satyanarayana, J.C. Dabrowiak, J.B. Chaires. *Biochemistry*, **32**, 2573 (1993).
[19] H.L. Wu, J.K. Yuan, Y. Bai, G.L. Pan, H. Wang, J. Kong, X.Y. Fan, H.M. Liu. *Dalton Trans.*, 8829 (2012).
[20] A.M. Pyle, J.P. Rehmann, R. Meshoyrer, C.V. Kumar, N.J. Turro, J.K. Barton. *J. Am. Chem. Soc.*, **111**, 3051 (1989).
[21] A. Wolfe, G.H. Shimer Jr, T. Meehan. *Biochemistry*, **26**, 6392 (1987).
[22] G.C. Baguley, M. Le Bret. *Biochemistry*, **23**, 937 (1984).
[23] J.R. Lakowicz, G. Weber. *Biochemistry*, **12**, 4161 (1973).
[24] C.P. Tan, J. Liu, L.M. Chen, S. Shi, L.N. Ji. *J. Inorg. Biochem.*, **102**, 1644 (2008).
[25] H.M.J. Hendriks, P.J.M.W.L. Birker, G.C. Verschoor, J. Reedijk. *J. Chem. Soc., Dalton Trans.*, 623 (1982).
[26] M. Pan, X.L. Zheng, Y. Liu, W.S. Liu, C.Y. Su. *Dalton Trans.*, 2157 (2009).
[27] Bruker. *SMART, SAINT and SADABS*, Bruker AXS Inc., Madison, WI (2000).
[28] G.M. Sheldrick. *SHELXTL*, Siemens Analytical X-ray Instruments Inc., Madison, Wisconsin (1996).
[29] W.J. Geary. *Coord. Chem. Rev.*, **7**, 81 (1971).
[30] W.K. Dong, G.H. Liu, Y.X. Sun, X.Y. Dong, X.H. Gao. *Naturforsch.*, **67b**, 17 (2012).
[31] M.S. Lah, H. Chun. *Inorg. Chem.*, **36**, 1782 (1997).
[32] A. Patra, S. Sen, S. Sarkar, E. Zangrando, P. Chattopadhyay. *J. Coord. Chem.*, **65**, 4096 (2012).
[33] H. Li, X.Y. Le, D.W. Pang, H. Deng, Z.H. Xu, Z.H. Lin. *J. Inorg. Biochem.*, **99**, 2240 (2005).
[34] V.G. Vaidyanathan, B.U. Nair. *Eur. J. Inorg. Chem.*, **19**, 3633 (2003).
[35] V.G. Vaidyanathan, B.U. Nair. *Eur. J. Inorg. Chem.*, **9**, 1840 (2004).
[36] J. Liu, T.X. Zhang, T.B. Lu, L.H. Qu, H. Zhou, Q.L. Zhang, L.N. Ji. *J. Inorg. Biochem.*, **91**, 269 (2002).
[37] H.L. Wu, J.K. Yuan, Y. Bai, G.L. Pan, H. Wang, X.B. Shu, G.Q. Yu. *J. Coord. Chem.*, **65**, 616 (2012).
[38] Q.H. Zhou, P. Yang. *Acta Chim. Sin.*, **64**, 793 (2006).
[39] S. Mahadevan, M. Palaniandavar. *Inorg. Chem.*, **37**, 693 (1998).
[40] A.B. Tossi, J.M. Kelly. *Photochem. Photobiol.*, **49**, 545 (1989).
[41] S. Satyanarayana, J.C. Dabrowiak, J.B. Chaires. *Biochemistry*, **31**, 9319 (1992).